

Cite this: DOI: 10.1039/xxxxxxxxxx

Supplementary Information for: How Interface Compatibility Affects Conductivity Evolution of Silver Nanobelts-filled Electrically Conductive Composites During Cure and Post-Treatments[†]

Geoffrey Rivers,^{*a} Pearl Lee-Sullivan,^a and Boxin Zhao^b

Received Date
Accepted Date

DOI: 10.1039/xxxxxxxxxx

www.rsc.org/journalname

Using silver nanobelts and silver microflakes in a DGEBA/TETA epoxy matrix, we sought to investigate the relationship between the evolving electrical resistivity of formulations of hybrid nanocomposites during the curing process. This was characterized using three methods: (i) *in-situ* four-wire electrical resistance measurements; (ii) differential scanning calorimetry, and (iii) dilatometry. In a previous work we reported that the resistivity of microcomposites was strongly affected by partial vitrification during curing. In this study, the reported vitrification effect is observed again, further validating the concern of far-ranging implications on the industry practices. The addition of silver nanobelts greatly improved conductivity of the composites, though it was observed that the improvements are often lost during subsequent heating and cooling cycles. Resistivity observations indicate that the sensitivity may be due to insufficient nanobelt-nanobelt contacts in the composite, and thus further increasing the nanobelt fraction of the filler content can maximize conductivity.

S1 Cure Conversion: Differential Scanning Calorimetry and Dilatometry

Calorimetry and dilatometry of the composites was performed. The cure conversion of the composites obtained by calorimetry, and the dimensional change *via* linear dilatometry during cure during the “ramp” heating condition are presented in Figure S1 a and b, respectively. Similarly, the cure conversion and dilatometry during the “Hold(T_g -30 °C)” and “Hold(T_g -15 °C)” heating conditions are presented, Figures S2, S3, and S4, corresponding to the 505, 601, and 603 formulations, respectively.

The calorimetry data obtained demonstrates that all specimens were cured to completion during the first heat treatment, since no further curing could be detected during the second heating cycle. There is little variation in the cure progression seen between the studied formulations, simplifying comparisons. The final glass transition temperatures ($T_{g\infty}$), listed in Table S1, include as much as a 15 °C reduction from the previously reported $T_{g\infty}$ for neat

DER-331/TETA epoxy, which was 135 °C. The differences in $T_{g\infty}$ do not correlate with the nanobelt content, and instead are likely due to the small and variable quantities of residual solvent remaining from composite preparation.

Dilatometry of the composites during cure and heating typically resulted in a net 1% contraction of the composites during the first half of curing, as seen in Figures S1 b), S2 b), S3 b), and S4 b). As the cure progressed the contraction slowed, and eventually was overcome by the thermal expansion of the composite. Often, small steps or kinks in the curve are present in the period prior to the test temperature reaching the $T_{g\infty}$ of the composite (as determined by calorimetry). For the Hold condition tests, it can be seen that the polymer is very slowly contracting during the isothermal period, indicating either contraction from slowly ongoing curing, slow relaxation of stored stress, or a combination of the two mechanisms.

S2 Cure and Glass Transition Calculations

The following Equation S2 was used to calculate the degree of conversion from the calorimetry data, based on the non-reversing heat flow (\dot{Q}_{NRFH}) obtained from applying modulated temperature conditions. For a particular heating, this was integrated over the full reaction to obtain the estimated “total heat of reaction” (ΔH_{tot}). An integral between time $t=j$ and time $t=i$ obtains the heat produced over that period. Starting with j equal to the on-

^a Department of Mechanical and Mechatronics Engineering, University of Waterloo, 200 University Ave, Waterloo, Ontario, Canada. Tel: +1 519 888 4567 ext 31671; E-mail: geoffrivers@gmail.com

^b Department of Chemical Engineering, University of Waterloo, 200 University Ave, Waterloo, Ontario, Canada.

[†] Related Main Manuscript available: [details of main document should be included here]. See DOI: 10.1039/b000000x/

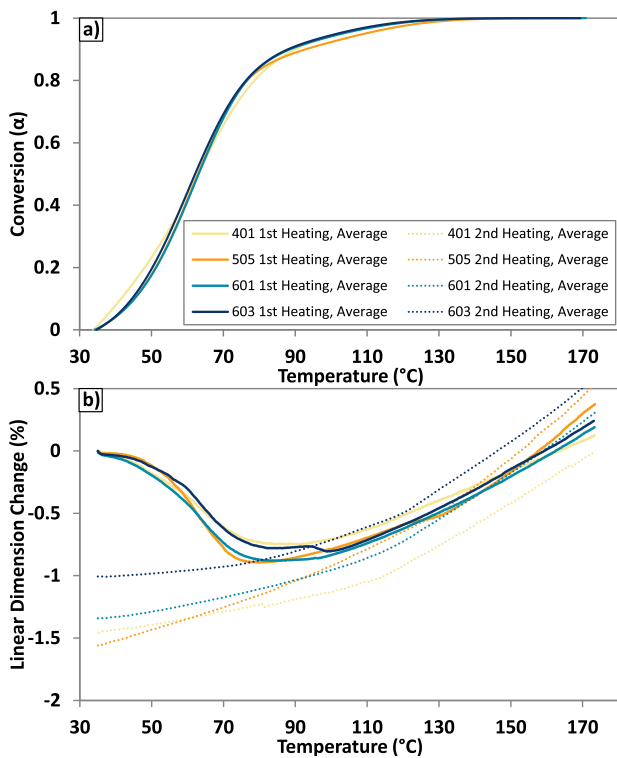


Fig. S1 a) Cure completion from calorimetry, and b) cure contraction via TMA, for four hybrid nanocomposites obtained during cure under continuous heating.

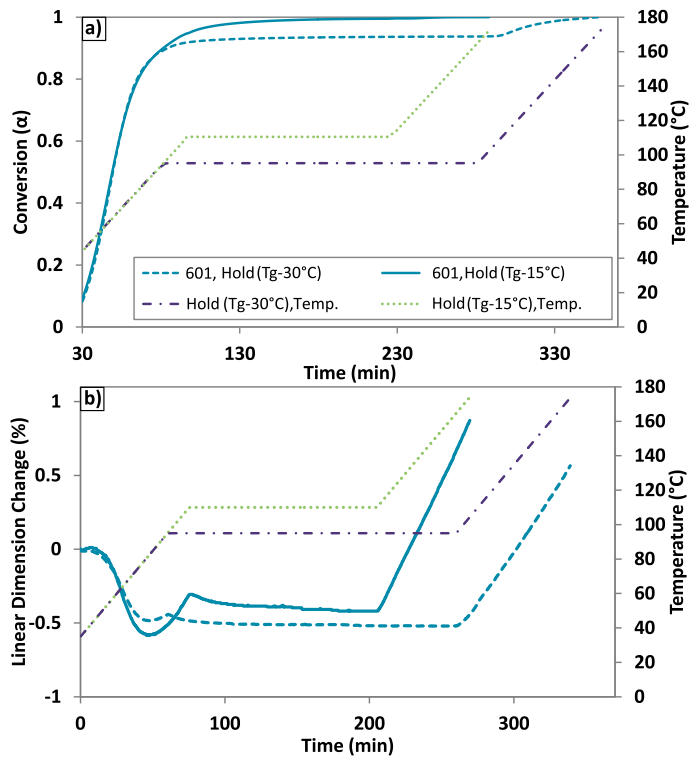


Fig. S3 a) Cure completion from calorimetry, and b) cure contraction via TMA, a hybrid nanocomposite 601 obtained during cure under the two isothermal Hold heat treatments.

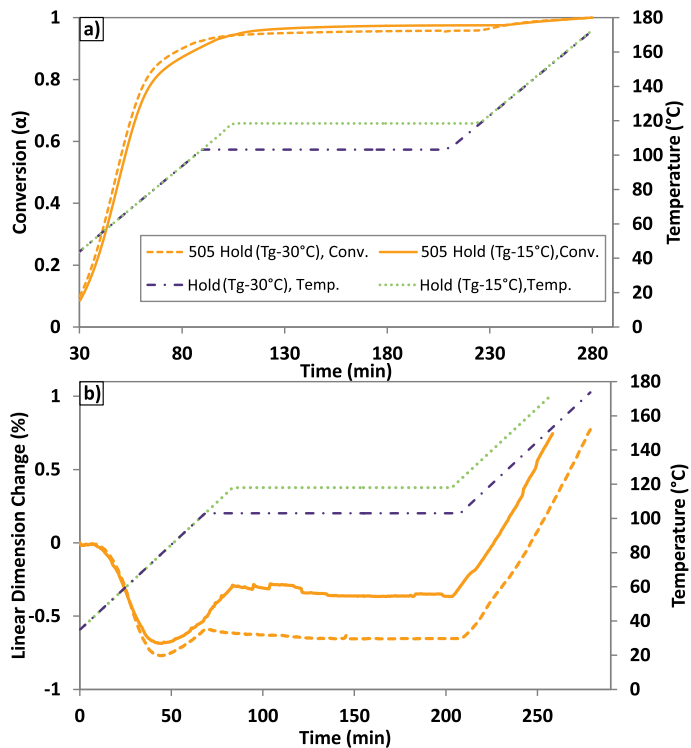


Fig. S2 a) Cure completion from calorimetry, and b) cure contraction via TMA, a hybrid nanocomposite (505) obtained during cure under the two isothermal Hold heat treatments.

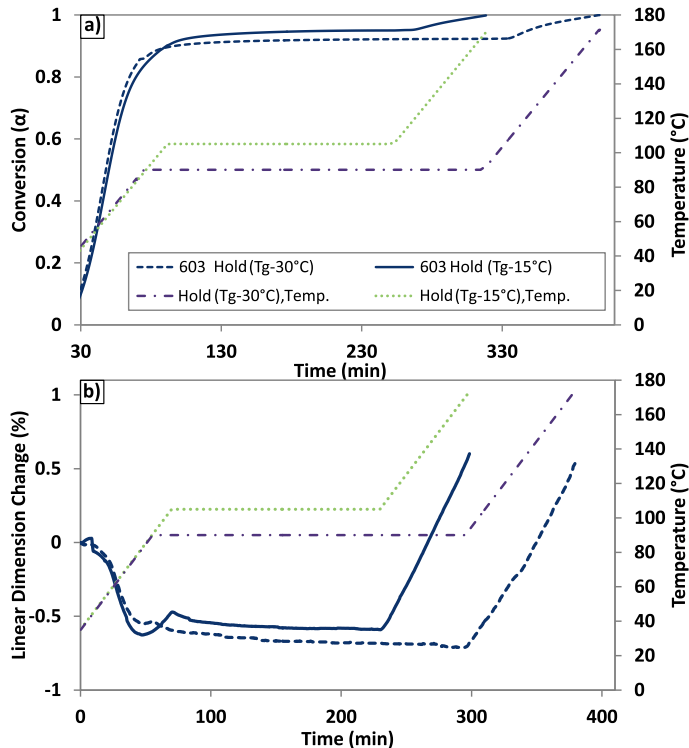


Fig. S4 a) Cure completion from calorimetry, and b) cure contraction via TMA, a hybrid nanocomposite 603 obtained during cure under the two isothermal Hold heat treatments.

Table S1 Key glass transition and conversion data for hybrid nanocomposites under continuous heating

Formulation Label	1(°C)/min Ramp	Condition
	$T_{g\infty}$ (°C)	$\alpha_{T_{g\infty}}$ %
401	122	98.9
505	134	99.2
601	126	99.2
603	120	98.8

set of the peak, and treating that as the start of the reaction, the “degree of cure” or “degree of conversion” at time i (α_i) is evaluated with Equation S2. The derivative of α_i is the instantaneous rate of conversion at some time and temperature. Integration of \dot{Q}_{NRFH} requires selection of a baseline. The simplest is a straight-line baseline from the onset of the peak to the apparent end of the reaction (characterized by the “onset” time at the end of the reaction). Analysis of the cure progression, rate, and heat-flow can reveal a wealth of information on their own, especially when comparing multiple heating conditions or material formulations.

$$\alpha_i = \frac{\int_{t=j}^{t=i} \dot{Q}_{NRFH} dt}{\Delta H_{Tot}} \quad (S2)$$

The more densely cross-linked the polymer is, the higher the range of temperatures needed to activate the cooperative movement. As such, as a thermoset cures its instantaneous T_g at that degree of conversion ($T_{g\alpha}$) will increase to its “maximum”, “final”, or “ultimate” T_g ($T_{g\infty}$). The glass transition is a second-order phase transition, and therefore occurs over a temperature range. It is accompanied, and identifiable, by a sigmoidal step change in the heat capacity of the material throughout the transition. This is apparent in the Reversing Heat Capacity ($RevC_p$) obtained from applying modulated temperature conditions. To obtain a single descriptive temperature for $T_{g\alpha}$ or $T_{g\infty}$, we take the temperature at which half the height of the sigmoidal change in heat capacity ($1/2\Delta C_p$) has occurred.

S3 Dilatometry Calculations

The initial thickness of each pair of slide covers (denoted by $y_{g,1}$) was measured at room temperature *via* TMA, prior to dispensing the composite specimen. Using these initial measurements, the thickness of the glass slides at each temperature (denoted by $y_{g,2}$) was calculated based on the coefficient of thermal expansion of the borosilicate glass slide covers used (Fisherbrand Cover Glasses, 12-542B). These values were subtracted from the total thickness measurements obtained by the TMA (y_1 and y_2), to obtain the composite thickness at each condition ($y_{c,1}$ and $y_{c,2}$). Changes in linear dimension are collected, and analyzed in terms of “percent change” from initial composite thickness. This can be seen in Equation S3:

$$\begin{aligned} \Delta l\% &= \frac{y_{c,2} - y_{c,1}}{y_{c,1}} \times 100 \\ &= \frac{(y_2 - y_{g,2}) - (y_1 - y_{g,1})}{(y_1 - y_{g,1})} \times 100 \end{aligned} \quad (S3)$$

$$\text{where...} y_{g,2} = (T_2 - T_1) \alpha_{borosilicateglass} y_{g,1},$$

S4 Resistance During Curing: Detailed view of Ramp Heat Condition

A detailed view of the data collected during cure, under the Ramp heating condition, is presented in Figure S5. This is an excerpt of Figure 3 of the main manuscript, presenting only the data from the first heating period during which cure went to completion. This data demonstrates that mid-cure there is a period during which the conductivity of the composite begins to develop, followed by the conductivity being disrupted temporarily. After that, the cure continues and the temperature increases, leading to the re-establishment and development of conductivity.

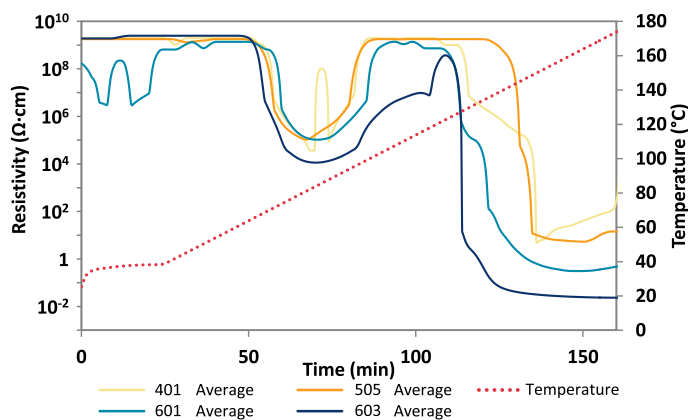


Fig. S5 Average resistivity data for four hybrid nanocomposites during curing, obtained during the initial continuous heating. This is an excerpt of Figure 3 of the main manuscript.

This is consistent with the results seen in a previous work by this group, investigating the onset of conductivity during cure for epoxy-based microcomposites filled with silver microflakes¹. Comparing the data to the cure data in Figure S1 a, it can be seen that the disruption is occurring during the partial vitrification of the composite during cure, above 80% conversion, just as was seen in the previous work¹.

Acknowledgements

The authors gratefully acknowledge financial support by the Refined Manufacturing Acceleration Process (ReMAP) program.

Notes and references

- 1 G. Rivers, P. Lee-Sullivan and B. Zhao, *Compos. Sci. Technol.*, 2017, **149**, 90 – 99.